

See discussions, stats, and author profiles for this publication at: <https://www.researchgate.net/publication/359080603>

# COVID-19 Identification Using Deep Capsule Network: A Perspective of Super-Resolution CNN on Low-Quality CXR Images

Conference Paper · December 2021

DOI: 10.1145/3507971.3507989

---

CITATIONS

3

READS

87

9 authors, including:



Grace U. Nneji

Oxford Brookes College of Chengdu University of Technology

48 PUBLICATIONS 447 CITATIONS

[SEE PROFILE](#)



Jianhua Deng

Peking Union Medical College Hospital

28 PUBLICATIONS 391 CITATIONS

[SEE PROFILE](#)



Happy Nkanta Monday

Oxford Brookes College of Chengdu University of Technology

53 PUBLICATIONS 584 CITATIONS

[SEE PROFILE](#)



Edidiong Christopher James

University of Electronic Science and Technology of China

13 PUBLICATIONS 151 CITATIONS

[SEE PROFILE](#)

# COVID-19 Identification Using Deep Capsule Network: A Perspective of Super-Resolution CNN on Low-Quality CXR Images

Grace U. Nneji\*

School of Information and Software Engineering, University of Electronic Science and Technology of China  
ugochinneji@std.uestc.edu.cn

Happy N. Monday

School of Computer Science and Engineering, University of Electronic Science and Technology of China  
mh.nkanta@std.uestc.edu.cn

Abel Z. Yutra

School of Information and Software Engineering, University of Electronic Science and Technology of China  
abelzenebe2014@gmail.com

Jingye Cai

School of Information and Software Engineering, University of Electronic Science and Technology of China  
jycail@uestc.edu.cn

Edidiong C. James

School of Information and Software Engineering, University of Electronic Science and Technology of China  
edianajames@yahoo.com

Yobsan B. Leta

School of Information and Software Engineering, University of Electronic Science and Technology of China  
yobsan23@gmail.com

Jianhua Deng

School of Information and Software Engineering, University of Electronic Science and Technology of China  
jianhua.deng@uestc.edu.cn

Bona D. Lemessa

School of Information and Software Engineering, University of Electronic Science and Technology of China  
bonadebela1989@gmail.com

Saifun Nahar

School of Computer and Information System, University of Missouri St louis MO, USA  
snnnm@umsl.com

## ABSTRACT

Chest X-ray has become a useful method in the detection of coronavirus disease-19 (COVID-19). Due to the extreme global COVID-19 crisis, using the computerized diagnosis method for COVID-19 classification upon CXR images could significantly decrease clinician workload. We explicitly addressed the issue of low CXR image resolution by using Super-Resolution Convolutional Neural Network (SRCNN) to effectively reconstruct high-resolution (HR) CXR images from low-resolution (LR) CXR correspondents. Then, the HRCXR images are fed into the modified capsule network to retrieve distinct features for the classification of COVID-19. We demonstrate the proposed model on a public dataset and achieve ACC of 97.3%, SEN of 97.8%, SPE of 96.9%, and AUC of 98.0%. This new conceptual framework is proposed to play a vital task in the issue facing COVID-19 and related ailments.

## CCS CONCEPTS

- Computing methodologies → Artificial intelligence; Computer vision; Computer vision problems; Object identification.

## KEYWORDS

Deep learning, chest x-ray, Convolutional Neural Network (CNN), COVID-19, capsule network, super-resolution

## ACM Reference Format:

Grace U. Nneji, Jingye Cai, Jianhua Deng, Happy N. Monday, Edidiong C. James, Bona D. Lemessa, Abel Z. Yutra, Yobsan B. Leta, and Saifun Nahar. 2021. COVID-19 Identification Using Deep Capsule Network: A Perspective of Super-Resolution CNN on Low-Quality CXR Images. In *2021 the 7th International Conference on Communication and Information Processing (ICCIPI) (ICCIPI 2021), December 16–18, 2021, Beijing, China*. ACM, New York, NY, USA, 7 pages. <https://doi.org/10.1145/3507971.3507989>

## 1 INTRODUCTION

COVID-19 is a transmissible respiratory disease spreading across the world [1]. As of November 12th, 2021, there had been over 5 million deaths and over 252 million confirmed cases [2]. Reverse Transcription Polymerase Chain Reaction (RT-PCR) is the golden standard for diagnosing COVID-19. However, this manual method of using throat swabs and nasopharyngeal are affected by small viral load and sample errors. More so, RT-PCR [3] is complex, takes much time, requires multiple tests for a definitive result and relatively low sensitivity. With the drawbacks of RT-PCR, computed tomography (CT) and chest X-ray (CXR) are other radiological techniques [4, 5] for identifying and assessing the seriousness of the virus. Despite the fact that CT imaging offers higher specificity and sensitivity [5], CXR imaging seems to be the norm in screening protocols because of its quickness, affordable, minimal invasive, and requires less logistical effort to implement.

Within the few years, several methods and DL frameworks for identification of COVID-19 based on CXR images and other medical dataset have been published with classification accuracies greater

Permission to make digital or hard copies of all or part of this work for personal or classroom use is granted without fee provided that copies are not made or distributed for profit or commercial advantage and that copies bear this notice and the full citation on the first page. Copyrights for components of this work owned by others than ACM must be honored. Abstracting with credit is permitted. To copy otherwise, or republish, to post on servers or to redistribute to lists, requires prior specific permission and/or a fee. Request permissions from [permissions@acm.org](mailto:permissions@acm.org).

ICCIPI 2021, December 16–18, 2021, Beijing, China

© 2021 Association for Computing Machinery.

ACM ISBN 978-1-4503-8519-0/21/12...\$15.00

<https://doi.org/10.1145/3507971.3507989>

than or equal to 90% [6] - [9]. In [10] a deep anomaly-based technique was used to identify COVID-19 and achieved sensitivity (SEN) of 96% and specificity (SPE) of 70%. Another study was conducted in [11] using CNN for feature extraction and LSTM for classification, 99% was achieved as the classification accuracy (ACC). Utilizing Pre-trained Xception architecture, the researchers of [12] adopted a design for COVID-19 identification achieving ACC of 97%. Another paper [13] proposed DarkCovidNet model for an early detection of COVID-19 case while using heatmaps to assist radiologists to segment the affected region in the CXR and achieved 98.07% and 87.03% ACC for binary and multiple classes respectively.

Khan et al. [14] presented a DCNN model based on pre-trained Xception architecture and achieved precision of 93.0%, ACC of 89.6% and recall rate of 98.2% for multi-class dataset. Four deep pre-trained CNN architectures were utilized in [15] achieving sensitivity of about 98% and specificity of approximately 93%. Five deep neural networks have achieved great performance in the identification of COVID-19, control and pneumonia images in [16] and achieved high ACC, SEN, SPE of 96.78%, 98.66%, and 96.46% respectively. Using the MobileNet-V2 network, an ACC of 96% was achieved for binary class, while 94% ACC was obtained for multi-class. A network trained from scratch and combined with a pre-trained network with fine-tuning for feature extraction was suggested in [17].

Above all, the DL methods are based on network algorithm variations, with little attention paid to the variability factors such as image resolution and quality which is a major concern and requires to be addressed before being implemented in medical environment. Furthermore, most state-of-the-art works have adopted deeper convolutional neural networks which could suffer gradient vanishing problem and loss of spatial details due to the max-pooling operation, thereby reducing the impact of the proposed approaches. With all these considerations, this article employed a super-resolution CNN model to improve the low resolution of the actual CXR images with no loss of restoration ACC and introducing a modified capsule network for the classification of COVID-19. The following is a breakdown of the paper's structure. The approach and proposed framework architecture is presented in section 2, while we conducted the experiment analysis in section 3. Finally, we presented relevant discussion and conclusion in section 4.

## 2 METHODOLOGY

This section introduces the super-resolution technique and our proposed network architecture.

### 2.1 Super-Resolution Network

SRCCN makes up the super resolution network which recaptures high-resolution images from low-resolution images. Patches are drawn out from the low-resolution image  $Y$ , and each patch is depicted as high-dimensional detail map. These high-dimensional vector feature maps are non-linearly mapped onto a high-dimensional vector representing a high resolution patch. Finally, the high resolution patch representations are aggregated to produce high-resolution images that closely resemble the ground truth  $X$ .  $F_1$  represents the patch extraction of the first convolutional sheet in Equation (1).

$$F_1(Y) = \max(0, W_1 * Y + B_1) \quad (1)$$

The filter and biases are denoted by  $W_1$  and  $B_1$ , respectively, and the convolutional operation is denoted by  $*$ . In this case,  $W_1$  contains  $n_1$  support  $c \times f_1 \times f_1$  filters, where  $c$  is the channel count in the input images and  $n_1$  is the filter's spatial size.  $F_2$  represents the nonlinear mapping activity of the high-dimensional vector function maps onto high-resolution patch of the second convolutional layer in Equation (2).

$$F_2(Y) = \max(0, W_2 * Y + B_2) \quad (2)$$

The filter and biases are denoted by  $W_2$  and  $B_2$ , respectively.  $W_2$  comprise of  $n_2$  filters of size  $n_2 \times f_2 \times f_2$ , and  $B_2$  is a two-dimensional array. Each  $n_2$ -dimensional vector function performance corresponds to a high-resolution piece required for reconstruction. The high-dimensional vector feature maps that represent the high-resolution patch are reconstructed into high-resolution images, which are denoted by the letters  $F$  in Equation (3).

$$F(Y) = W_3 * F_2(Y) + B_3 \quad (3)$$

Here,  $W_3$  equals to  $c$  filters of size  $n_2 \times f_3 \times f_3$  and  $B_3$  corresponds to  $c$ -dimensional vector.

### 2.2 Network Architecture and Implementation

For classification problems, the authors in [18] were the first to propose capsule network. Unlike traditional CNNs, which use scalar-oriented neurons to represent the likelihood of the presence of various attributes, the capsule network is built up of entity-aligned vectorial capsules. In retrieving intrinsic and distinguishing properties of entities, capsule networks are far more stronger and robust than ordinary CNNs [18, 19].

A key characteristic of this capsule formulation which is impossible to achieve with CNN scalar neuron models is that the vectorial orientation permits a capsule to learn and detect variants of a feature. The overall input in the convolutional capsule layers is the weighted summation of all predictions gotten from the capsules inside the convolutional kernel as seen in Equation (4).

$$C_j = \sum_i a_{ij} \cdot U_{j/i} \quad (4)$$

Where  $C_j$  represents the sum total input to capsule  $j$ ; the indicator that depicts the degree of which capsule  $i$  activates capsule  $j$  is called the coupling coefficient  $a_{ij}$ ,  $U_{j/i}$ . The prediction  $U_{j/i}$  from capsule  $i$  to capsule  $j$  is illustrated below in Equation (5).

$$U_{j/i} = W_{ij} \cdot U_i \quad (5)$$

$U_i$  denotes the capsule  $i$ 's output and  $W_{ij}$  represents the weight network on the edge linking capsules  $i$  and  $j$ . A robust routing method [19] decide the coefficient between capsule  $i$  and other linked capsules in the above layer summing to 1. To ignite another capsule, the robust routing method called routing by agreement considers both the length of a capsule and its instantiation parameters. This differs from traditional CNN models which simply evaluate probability. As a result, capsule networks are reliable and more powerful at abstracting inherent object characteristics. Recollect that the capsule's length is used to determine the likelihood of an entity's presence. Non-linear "squashing" function activates the convolutional capsule layers in ensuring a perfect probability

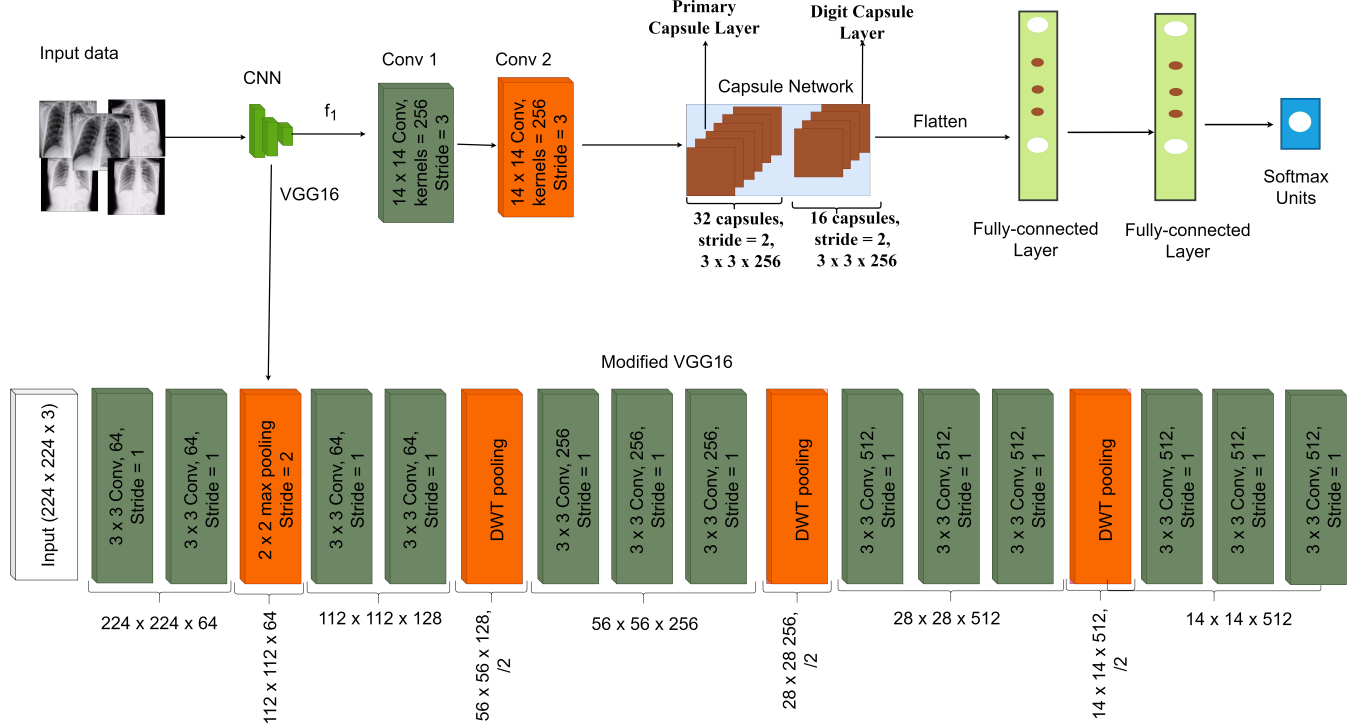


**Figure 1: Our proposed capsule network with wavelet pooling for COVID-19 Classification**

estimation where short vectorial capsules have low likelihood, otherwise high probability for the purpose of maintaining a constant orientation. Squashing function is given in Equation (6).

$$U_j = \frac{\|C_j\|^2}{1 + \|C_j\|^2} \cdot \frac{C_j}{\|C_j\|} \quad (6)$$

In this study, the input size of the super-resolution images are resized to  $224 \times 224 \times 3$  and fed into network. We utilized VGG16 model as the feature extractor due to its reasonable network depth without performance degradation and better results on image classification task. VGG16 has 13 convolutional layers arranged in blocks, 3 fully connected layers and 5 max-pooling layers. To achieve better classification performance and maintain the integrity of high-level features, it is necessary to extract the high-level features of the CXR images by removing the max-pooling layers in the second, third, fourth and fifth blocks and replace it with discrete wavelet transform (DWT) pooling layers in order to reduce the loss of spatial details to the minimum so as to achieve reduction in dimension without losing positional details. More so, The 3 fully connected layers are removed and the max-pooling layer in the fifth block is also removed without replacement in order to arrive at an output of  $14 \times 14 \times 512$  feature vector. Furthermore, to preserve the spatial details of the high-level extracted features,  $f_1$  and to reduce the vector dimension as well as to maintain dimensionality match with the primary convolutional capsule layer, we added 2 convolutional layers of  $14 \times 14$  with kernel size of 256 and stride of 3.

Thereafter, the spatial details are transformed into Primary Capsule layers (PrimaryCaps) in form of capsules after the feature extraction stage. Also, the max-pooling layer in capsule performs feature down-sampling in order to reduce the network size. However, we adopted DWT pooling of  $K_m \times K_m$  to replace max-pooling layer and stride of  $K_m$  direct to the feature maps of the last convolutional capsule layer. Only capsule with the longest vector are kept while the rest are discarded in the  $K_m \times K_m$  kernel. To this effect, the size of the network and capsule number are reduced and leaving a selection of the essential capsules. Routing by agreement is introduced to learn the spatial details in form of transformation matrix. The connection strength of the digit capsule is controlled by the routing coefficient. A high-level entity abstraction with a global view is flatten to arrive at the feature embeddings.

More so, dynamic routing between two connected capsule layers is utilized and the squashing function is used to normalize capsule outputs. The probability that the capsule instance exists is represented by the length of the feature vector which is compressed to 1 with the help of a non-linear function. We added a convolutional layer to the network in order to reduce the dimension. We introduce a regularization term to enhance the robustness of the model. Then, these embedding features are connected with a fully-connected (FC) layer for feature integration and the network will decide using the last FC layer as a softmax classifier to predict the result. The overall architecture of the proposed capsule network is presented in Figure 1.

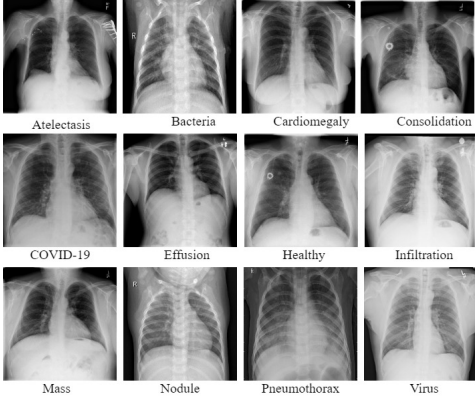


**Figure 2: COVID-19, healthy and other pneumonia related CXR sample images**

### 3 EXPERIMENTAL RESULTS AND DISCUSSION

#### 3.1 Model Hyper-Parameters

In this study, we trained our model for COVID-19 classification using a modified capsule network while using an Adam optimizer and dropout to avoid over-fitting, early stop techniques and a learning rate of 0.0001 in order to obtain an effective model with better performance. In this work, we have examined how the model performance can be influenced by tuning some hyper-parameters such as dropout, pooling method, learning rate (LR), batch normalization (BN) and optimizer (Adam). Also, we applied some evaluation metrics in terms of ACC, SEN, SPE and AUC on our proposed model.

#### 3.2 Dataset

We gathered our data from two publicly source datasets for this investigation. COVID-19 dataset was obtained from [20]. It's worth noting that all of our COVID-19 CXR comes from this dataset, which has 250 COVID-19 CXR. We ended up with 162 COVID-19 CXR scans after cleaning and sorting, since only images with detectable radiographic signals are maintained, while all other CXRs are eliminated. Our second dataset came from the NIH dataset [21], which included scans of different pneumonia illnesses as well as healthy images. Table 1 displays the number of CXR images in the training and test sets, whereas Figure 2 depicts the CXR image distribution in our dataset, which includes COVID-19, healthy, and various pneumonia-related illnesses.

#### 3.3 Performance Measures

We have applied some evaluation metrics in terms of AUC, SEN, SPE, ACC and specificity on our proposed model. Equation (7) – Equation (9) are the provided equation for the evaluation metrics.

$$\text{Accuracy(ACC)} = \frac{TN + TP}{FP + TN + TP + FN} \quad (7)$$

$$\text{Sensitivity(SEN)} = \frac{TP}{FN + TP} \quad (8)$$

**Table 1: Description of the Dataset**

Dataset	Training Set	Test Set	Total
Atelectasis	130	32	162
Bacteria	130	32	162
Cardiomegaly	130	32	162
Consolidation	130	32	162
COVID-19	130	32	162
Effusion	130	32	162
Healthy	130	32	162
Infiltration	130	32	162
Mass	130	32	162
Nodule	130	32	162
Pneumothorax	130	32	162
Virus	130	32	162
Total	1,560	384	

**Table 2: Performance comparison with other state of the art models with our proposed model**

Model	ACC (%)	SEN (%)	SPE (%)
Song et al. [22]	86.0	96.0	77.0
Tang et al. [23]	87.5	93.3	74.5
Wang et al. [24]	93.3	91.4	90.5
Zheng et al. [25]	90.1	90.7	91.1
Shi et al. [26]	89.4	90.7	87.2
Jin et al. [27]	95.2	97.4	92.2
Xu et al. [28]	86.7	87.9	90.7
<b>Ours</b>	<b>97.3</b>	<b>97.8</b>	<b>96.9</b>

**Table 3: Performance comparison of our proposed model with selected pre-trained models.**

Model	ACC (%)	SEN (%)	SPE (%)	AUC (%)
DenseNet	94.7	95.2	94.8	95.1
ResNet-101	95.4	94.8	95.6	94.8
MobileNet V3	95.3	94.9	95.2	95.7
EfficientNet	95.9	95.7	94.9	95.3
<b>Ours</b>	<b>97.3</b>	<b>97.8</b>	<b>96.9</b>	<b>98.0</b>

$$\text{Specificity(SPE)} = \frac{TN}{FP + TN} \quad (9)$$

#### 3.4 Result Analyses

Peak Signal to Noise Ration (PSNR) and Structural Similarity Index Metric (SSIM) are two important metrics for the evaluation of image reconstruction and enhancement. Figure 3 illustrates the performance of the super-resolution network in terms of PSNR and SSIM trained on Chest x-ray dataset, thus obtaining a satisfactory improvement in PSNR value of 32.85db and the SSIM of 0.9308. The PSNR value is reported on the left and SSIM is on the right as presented in Figure 3. Our proposed model has illustrated some

**Table 4: Performance evaluation of our proposed model based on different hyper-parameter tuning on our dataset with Adam optimizer.**

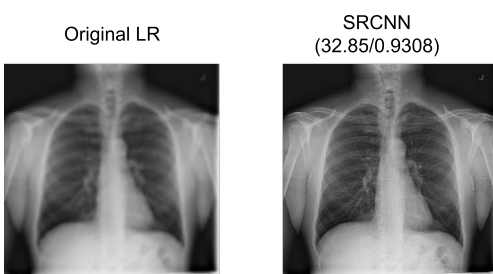
Hyper-parameter	Proposed model +	Proposed model +
	Wavelet pool +	Max-pool +
	BN + Adam	BN + Adam
Accuracy (%)	Accuracy (%)	
LR (0.0001) + Dropout (0.25)	95.9	94.4
LR (0.0001) + Dropout (0.50)	97.3	95.8
LR (0.0001) + Dropout (0.75)	96.1	95.1

**Table 5: Performance evaluation of our proposed model based on different hyper-parameter tuning on our dataset with Root Mean Square Propagation (RMSProp) optimizer.**

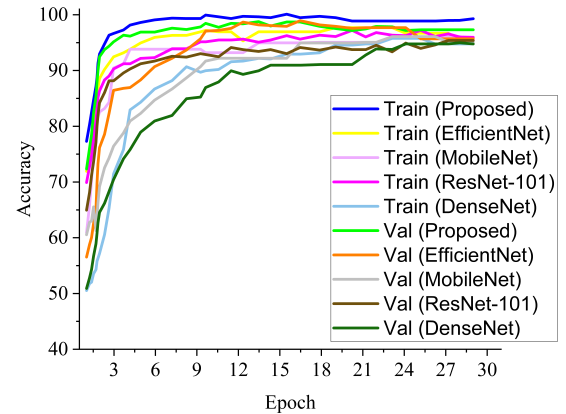
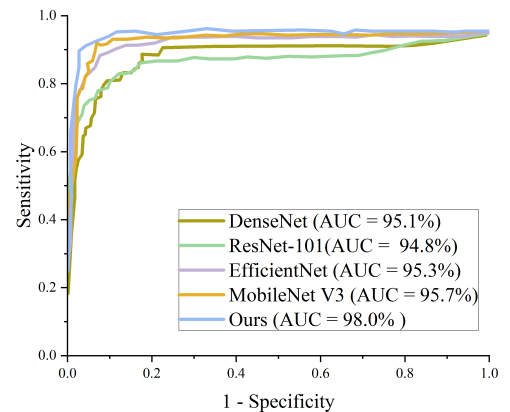
Hyper-parameter	Proposed model +	Proposed model +
	Wavelet pool +	Max-pool +
	BN + RMSProp	BN + RMSProp
Accuracy (%)	Accuracy (%)	
LR (0.0001) + Dropout (0.25)	96.1	94.3
LR (0.0001) + Dropout (0.50)	95.3	93.6
LR (0.0001) + Dropout (0.75)	94.9	93.1

**Table 6: Performance evaluation of our proposed model based on different hyper-parameter tuning on our dataset with Stochastic Gradient Descent (SGD) optimizer.**

Hyper-parameter	Proposed model +	Proposed model +
	Wavelet pool +	Max-pool +
	BN + SGD	BN + SGD
Accuracy (%)	Accuracy (%)	
LR (0.0001) + Dropout (0.25)	94.2	92.6
LR (0.0001) + Dropout (0.50)	94.7	91.7
LR (0.0001) + Dropout (0.75)	92.9	90.2

**Figure 3: Quantitative results of the SRCNN on CXR dataset. The PSNR value is reported on the left while the SSIM value is reported on the right for the whole region.****Table 7: The Distribution of Relabeled Data**

Label	Class	Number	Percentage
0	No RDR	548	45.6%
1	RDR	652	54.4%

**Figure 4: Training and validation curves showing the performance of our proposed model and the pre-trained models.****Figure 5: ROC showing the performance of our proposed model and the following pretrained models.**

performance results in Figure 4. Figure 4 displays the validation ACC and training ACC of the capsule network and the other models. However, our proposed model performs better than the other models with a higher margin, thus making our model have greater potential in clinical application. Another important metric is the Receiver Operating Characteristics (ROC) curve. The ROC curve measures the overall ACC in terms of AUC as shown in Figure 5, indicating that our model demonstrates a satisfactory balance between sensitivity and specificity by minimizing the error rate of the false positive and maximizing the true positive rate. Table 2 shows a comparative study of other researches for COVID-19 classification and it illustrates that our method outperforms other models. Table 3 presents the performance comparison of our proposed capsule network with selected pre-trained models in terms of ACC, SEN, SPE and AUC. The result indicates that our proposed algorithm is effective. It is worth mentioning that our proposed model performs optimally to hyper-parameter tuning as depicted in Table 4.

**Table 8: Comparison of our model with selected pre-trained model on the MESSIDOR dataset**

Model	ACC (%)	SEN (%)	SPE (%)	AUC (%)	Time (min)
ResNet-50	96.8	96.7	95.9	95.4	20.7
Inception V3	96.1	95.0	95.9	96.2	21.6
MobileNet V2	95.6	96.1	95.2	95.9	19.5
<b>Ours</b>	<b>97.3</b>	<b>97.9</b>	<b>98.6</b>	<b>98.8</b>	<b>18.2</b>

**Table 9: The Evaluation Result of the proposed Network with and without super resolution (SR)**

Model	ACC (%)	SEN (%)	SPE (%)	AUC (%)
Proposed network without SR model	95.9	95.7	96.6	95.3
Proposed network with SR model	97.3	97.9	98.6	98.8

## 4 DISCUSSION AND CONCLUSION

An efficient COVID-19 classification using a modified capsule network has been proposed. This involved the enhancing of the COVID-19 CXR dataset using the super-resolution CNN technique and modified capsule network using pre-trained VGG16 as the backbone for the classification of COVID-19. The evaluation results show that the proposed model achieves better performance with the ACC of 97.3%, sensitivity of 97.8%, specificity of 96.9%, and AUC of 98%. These results could effectively assist the radiologists to diagnose COVID-19 from other pneumonia-related diseases while saving screening time.

We conducted ablation study to examine how hyper-parameter tuning can enhance the performance of our proposed capsule network model. Different optimizer were examined at different learning rate and dropout as depicted in Table 4, Table 5, and Table 6. It is clear that Adam optimizer at a learning rate of 0.0001 and dropout of 0.50 achieved the highest ACC of 97.3% according to Table 4. It is worth mentioning that Adam optimizer is far more robust compared to the other optimizer (RMSProp and SGD) due to its computational efficiency.

More so, on the verge to further evaluate the wide application of our proposed network on other medical diseases, we considered a common medical disease known as retinopathy. In this case, we considered a two category of our dataset which is retinopathy with referable diabetes symptoms and non-referable diabetic symptoms as presented in Table 7. Table 8 shows the effectiveness of our proposed network in comparison with selected pre-trained models when applied to other medical disease. For the same hyper-parameter tuning, our proposed model achieved satisfactory performance when applied to retinopathy disease from fundus images as seen in Table 8. Table 9 presents the results in terms of ACC, SEN, SPE, AUC, and the computational time of our proposed capsule network with super resolution model and without super resolution model.

It is worth mentioning how our proposed model is different from the other models presented in Table 2. The utilization of pooling layers for down-sampling operations usually lead to loss of spatial details. However, it is obvious that the decline in performance of the other models is attributed to the loss of spatial details during the high-level feature extraction stage which in the case of our

proposed model, the high-level features are preserved. More to the point, traditional capsule network do not utilize pooling layers and as a consequence, more computational time is required and the dimensionality of the features are increased when compared to traditional CNN models but achieves higher ACC. To address the bottleneck associated with computational time of capsule network, we introduced wavelet pooling as an effective down-sampling operation that reduces the dimensionality of the features and at the same time, prevent the loss of spatial details. Additionally, our proposed model has a computational time that is much lower than most of the traditional pre-trained CNN models as compared in Table 8.

Our future work will seek to experiment more works by considering the following:

- Applying other hyper-parameter tuning technique while having more dataset size.
- Applying the same technique on other medical diseases.

## REFERENCES

- [1] T. Ai et al., "Correlation of chest CT and RT-PCR testing for coronavirus disease 2019 (COVID-19) in China: a report of 1014 cases," *Radiology*, vol. 296, no. 2, pp. E32–E40, 2020.
- [2] "COVID-19 Map - Johns Hopkins Coronavirus Resource Center." <https://coronavirus.jhu.edu/map.html> (accessed Nov. 27, 2021).
- [3] Y. Fang et al., "Sensitivity of chest CT for COVID-19: comparison to RT-PCR," *Radiology*, vol. 296, no. 2, pp. E115–E117, 2020.
- [4] T. Hu, Y. Liu, M. Zhao, Q. Zhuang, L. Xu, and Q. He, "A comparison of COVID-19, SARS and MERS," *PeerJ*, vol. 8, p. e9725, 2020.
- [5] G. U. Nneji et al., "A Super-Resolution Generative Adversarial Network with Siamese CNN Based on Low Quality for Breast Cancer Identification," in 2021 4th International Conference on Pattern Recognition and Artificial Intelligence (PRAI), 2021, pp. 218–223, doi: 10.1109/PRAI53619.2021.9551033.
- [6] H. N. Monday et al., "The Capability of Multi Resolution Analysis: A Case Study of COVID-19 Diagnosis," in 2021 4th International Conference on Pattern Recognition and Artificial Intelligence (PRAI), 2021, pp. 236–242, doi: 10.1109/PRAI53619.2021.9550802.
- [7] X. Xie, Z. Zhong, W. Zhao, C. Zheng, F. Wang, and J. Liu, "Chest CT for typical coronavirus disease 2019 (COVID-19) pneumonia: relationship to negative RT-PCR testing," *Radiology*, vol. 296, no. 2, pp. E41–E45, 2020.
- [8] G. U. Nneji et al., "Enhancing Low Quality in Radiograph Datasets Using Wavelet Transform Convolutional Neural Network and Generative Adversarial Network for COVID-19 Identification," in 2021 4th International Conference on Pattern Recognition and Artificial Intelligence (PRAI), 2021, pp. 146–151, doi: 10.1109/PRAI53619.2021.9551043.
- [9] H. N. Monday et al., "Improved Convolutional Neural Multi-Resolution Wavelet Network for COVID-19 Pneumonia Classification," in 2021 4th International Conference on Pattern Recognition and Artificial Intelligence (PRAI), 2021, pp. 267–273, doi: 10.1109/PRAI53619.2021.9551095.
- [10] J. Zhang et al., "Viral Pneumonia Screening on Chest X-rays Using Confidence-Aware Anomaly Detection," *IEEE Trans. Med. Imaging*, 2020.
- [11] M. Z. Islam, M. M. Islam, and A. Asraf, "A combined deep CNN-LSTM network for the detection of novel coronavirus (COVID-19) using X-ray images," *Informatics Med. Unlocked*, vol. 20, p. 100412, 2020.
- [12] N. N. Das, N. Kumar, M. Kaur, V. Kumar, and D. Singh, "Automated deep transfer learning-based approach for detection of COVID-19 infection in chest X-rays," *Irbn*, 2020.
- [13] T. Ozturk, M. Talo, E. A. Yildirim, U. B. Baloglu, O. Yildirim, and U. R. Acharya, "Automated detection of COVID-19 cases using deep neural networks with X-ray images," *Comput. Biol. Med.*, vol. 121, p. 103792, 2020.
- [14] A. I. Khan, J. L. Shah, and M. M. Bhat, "CoroNet: A deep neural network for detection and diagnosis of COVID-19 from chest x-ray images," *Comput. Methods Programs Biomed.*, vol. 196, p. 105581, 2020.
- [15] S. Minaee, R. Kafieh, M. Sonka, S. Yazdani, and G. J. Soufi, "Deep-covid: Predicting covid-19 from chest x-ray images using deep transfer learning," *Med. Image Anal.*, vol. 65, p. 101794, 2020.
- [16] I. D. Apostolopoulos and T. A. Mpetsiana, "Covid-19: automatic detection from x-ray images utilizing transfer learning with convolutional neural networks," *Phys. Eng. Sci. Med.*, vol. 43, no. 2, pp. 635–640, 2020.
- [17] I. D. Apostolopoulos, S. I. Aznaouridis, and M. A. Tzani, "Extracting possibly representative COVID-19 biomarkers from X-ray images with deep learning

- approach and image data related to pulmonary diseases,” *J. Med. Biol. Eng.*, p. 1, 2020.
- [18] S. Sabour, N. Frosst, and G. E. Hinton, “Dynamic routing between capsules,” *arXiv Prepr. arXiv1710.09829*, 2017.
- [19] M. E. Paoletti et al., “Capsule networks for hyperspectral image classification,” *IEEE Trans. Geosci. Remote Sens.*, vol. 57, no. 4, pp. 2145–2160, 2018.
- [20] J. P. Cohen, P. Morrison, L. Dao, K. Roth, T. Q. Duong, and M. Ghassemi, “Covid-19 image data collection: Prospective predictions are the future,” *arXiv Prepr. arXiv2006.11988*, 2020.
- [21] “NIH Chest X-rays | Kaggle.” <https://www.kaggle.com/nih-chest-xrays/data> (accessed Jun. 09, 2021).
- [22] Y. Song et al., “Deep learning enables accurate diagnosis of novel coronavirus (COVID-19) with CT images,” *IEEE/ACM Trans. Comput. Biol. Bioinforma.*, 2021.
- [23] Z. Tang et al., “Severity assessment of coronavirus disease 2019 (COVID-19) using quantitative features from chest CT images,” *arXiv Prepr. arXiv2003.11988*, 2020.
- [24] L. Wang, Z. Q. Lin, and A. Wong, “Covid-net: A tailored deep convolutional neural network design for detection of covid-19 cases from chest x-ray images,” *Sci. Rep.*, vol. 10, no. 1, pp. 1–12, 2020.
- [25] C. Zheng et al., “Deep learning-based detection for COVID-19 from chest CT using weak label,” *MedRxiv*, 2020.
- [26] F. Shi et al., “Large-scale screening to distinguish between COVID-19 and community-acquired pneumonia using infection size-aware classification,” *Phys. Med. & Biol.*, vol. 66, no. 6, p. 65031, 2021.
- [27] S. Jin et al., “AI-assisted CT imaging analysis for COVID-19 screening: Building and deploying a medical AI system in four weeks,” *MedRxiv*, 2020.
- [28] X. Xu et al., “A deep learning system to screen novel coronavirus disease 2019 pneumonia,” *Engineering*, vol. 6, no. 10, pp. 1122–1129, 2020.
- [29] “Messidor - ADCIS.” <https://www.adcis.net/en/third-party/messidor/> (accessed Nov. 27, 2021).